

Influences of source displacement on the features of subwavelength imaging of a photonic crystal slab

Pi-Gang Luan, Chen-Yu Chiang, Hsiao-Yu Yeh
*Wave Engineering Laboratory, Department of Optics and Photonics,
National Central University, Jhugli 320, Taiwan*

In this paper we study the characteristics of subwavelength imaging of a photonic crystal (PhC) superlens under the influence of source displacement. For square- and triangular-lattice photonic crystal lenses, we investigate the influence of changing the lateral position of a single point source on the imaging uniformity and stability. We also study the effect of changing the geometrical center of a pair of sources on the resolution of the double-image. Both properties are found to be sensitive to the displacement, which implies that a PhC slab cannot be treated seriously as a flat lens. We also show that by introducing material absorption into the dielectric cylinders of the PhC slab and widening the lateral width of the slab, the imaging uniformity and stability can be substantially improved. This study helps us to clarify the underlying mechanisms of some recently found phenomena concerning imaging instability.

PACS numbers: 78.20.Ci, 42.70.Qs, 42.25.Fx

I. INTRODUCTION

Since John Pendry [1] proposed that a perfect lens can in principle be designed to overcome the diffraction limit [2], issues concerning subwavelength imaging have become very important and popular [3–20]. A device that can focus the light from a point source into a spot of subwavelength width is called a superlens. Two kinds of superlens have been studied most. The first is a slab of left-handed metamaterial with appropriate negative permittivity and permeability, both close to -1 [1, 3–6]. The second is a slab of photonic crystal (PhC) with properly chosen band structure and equal-frequency contour (EFC) [8–17]. Both structures are recognized by most researchers as examples of flat lens, which means they have the advantage of having no optical axis. In fact, there are also structures which fall between the above categories, namely, the Mie-resonance based artificial structures operating in the subwavelength regime [21, 22], however, in this paper we will focus our attention only on the previous two categories. The transmission characteristics of the metamaterial slab can be explained with the effective theory of the metamaterial medium, whereas the electromagnetic behaviors of the PhC slab can only be understood through a detailed analysis of the PhC band structure. The comparison between them reveals that, although these two kinds of superlens have similar functions in focusing light and both consist of periodically arranged elements such as resonators and dielectric rods, they are in fact belonging to two different categories and should be distinguished carefully. One main difference might be that for a specific operating wavelength of subwavelength imaging, the corresponding lattice constant in the former structure is usually smaller than in the latter. Typically the operation wavelength of a PhC slab lens is about 3 to 5 times of the lattice constant. This indicates that a PhC slab is not a flat lens rigorously, and the non-uniformity of the structure should be considered carefully because it may have observable effects on the subwavelength imaging phenomena.

Previous studies have revealed that the surface waves decaying away from the PhC surface usually play important role in the subwavelength imaging [16, 17]. Since surface waves are transversely localized Bloch waves guided along a PhC surface, they must carry the information that manifests the surface structure (i.e., the arrangement of rods or holes and the way of termination) of the PhC. Now, if subwavelength images are located near the PhC surface, then both the surface structure and the sources position can influence the features of the images. The influences of surface termination have already been studied in Ref.[13, 16]. Recently, the effects of source displacement on the subwavelength imaging have also been found in the studies concerning the subwavelength imaging in photonic crystal lens [18] and photonic quasicrystal lens [19]. According to these studies, researchers found that the laterally displacement of the source can influence the image performance substantially. In fact, similar effect in acoustic imaging system had already been reported previously [20].

In this paper, we further study the influences of the source position on the subwavelength imaging of a PhC lens. For square-lattice and triangular-lattice PhCs consisting of dielectric cylinders, we first investigate the influence of changing the lateral position of a point source on the uniformity and stability of the single image. We then study the effects of moving the geometrical center of a pair of sources on the resolution of the double-image. We also discuss how to improve the imaging quality by including absorption effect into the dielectric cylinders consisting the PhC superlens.

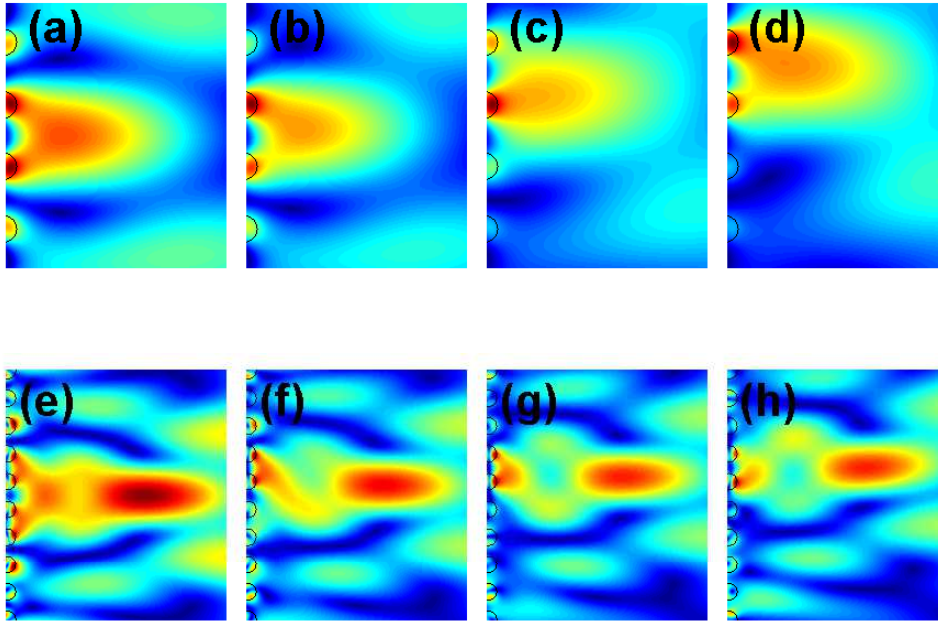


FIG. 1: The image field patterns (the absolute value of the \mathbf{E} fields) for the TM waves. Plots from (a) to (d) are for the square lattice cases of lateral source position: 0 , $\sqrt{2}a/3$, $2\sqrt{2}a/3$, and $\sqrt{2}a$. Plots from (e) to (h) are for the triangular lattice cases of lateral source positions: 0 , $a/3$, $2a/3$, and a .

II. PHENOMENA AND DISCUSSION

We first study the imaging characteristics of a square lattice slab consisting of dielectric cylinders in air background. In this paper only the TM (E-polarized) wave will be studied. The dielectric permittivity of the cylinders is $\epsilon = 14$, and the cylinder radius is $r_0 = 0.3a$, here a is the lattice constant. The slab has 8 layers in the x direction and 21 layers in the y (lateral) direction. The orientation of the air-PhC interfaces (slab surfaces) are ΓM . The dimensionless frequency $\omega a/2\pi c$ of the source is 0.192 , which is in the all-angle negative refraction frequency range [8]. In the beginning, the x -coordinate of the source is $0.5a$ away from the front (left) surface of the slab, located on x axis ($y = 0$), which is the symmetric axis of the slab. Note that the source-slab distance ($0.5a$) is only about one-tenth of the wavelength ($5.2a$), thus any kind of near field effect caused by the evanescent waves may play important role in the imaging process [17]. Fig 1.(a) is the electric field pattern (absolute value) of the image behind the back surface of the slab before we move the source. Now we keep the distance between the source and the front surface of the slab fixed, and move the source along the lateral direction. We notice that the image peak is not always located on the original image plane, especially in the cases 1(b) and 1(c). Even when the source has been moved one lateral period of distance $\sqrt{2}a$, the image field pattern does not recover its original form. In the second case we consider triangular lattice PhC slab. The results of this case are shown in figure 1(e) to 1(h). Again, the dielectric cylinders are embedded in the air background and the cylinder parameters are the same as in the square lattice case except that now the PhC-air interfaces are along the ΓK direction and the dimensionless source frequency is 0.335 , in the negative refraction range of the frequency [13]. The source is located $3.7a$ from the front interface, longer than one wavelength ($2.99a$). This means that the evanescent waves do not contribute much to the focused image. In figures 1(e) to 1(h) we find that the image peak always keeps staying on the same image plane and the symmetrical field pattern around the peak is almost uninfluenced when the source position has been changed.

When changing the source position along the lateral direction, two interesting features are found. The first is about the periodicity of the image strength curve and the other is about the homogeneity of the peak strength under the source movement. For a specific position of the source, the corresponding position and the strength of the image peak (maximum) is recorded and designated as, for example, an o sign. We then move the source laterally to a nearby point and record the new position and strength of the peak. After doing this operation many times, we collect a lot of data about the strength and position of the image peak. We can then fit these data with a smooth curve, and

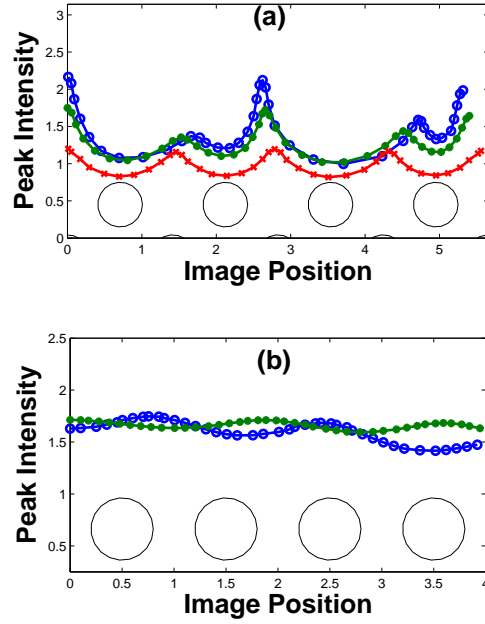


FIG. 2: The image peak intensity v.s. the source position. (a) The results for the square lattice cases. The source changing its position continuously from the central position $y = 0$ to a maximum lateral distance $y = 4\sqrt{2}a$ is shown in the plot (blue o). The results for an absorptive slab (red x) and a laterally-wider slab (51 cylinders along the lateral direction) (green *) are also shown. In calculating the results of the absorptive case, we choose $\epsilon = 14 + 0.2i$. (b) The results for the triangular lattice cases. The source changing its position continuously from $y = 0$ to $y = 4a$ is shown (blue o). The result for a wider (51 laterally arranged cylinders) slab is also shown (green *).

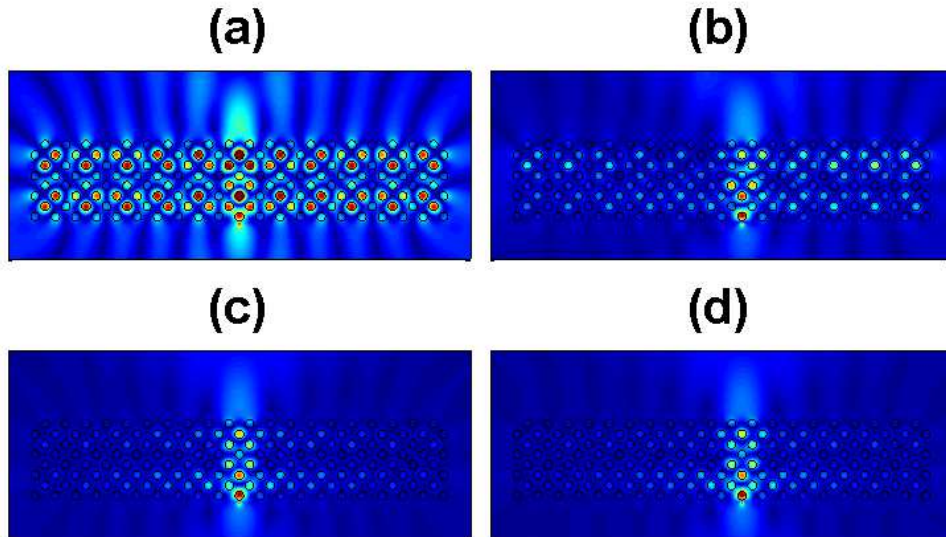


FIG. 3: The field patterns (the absolute value of the \mathbf{E} fields) for a 21-layer wide slab lens. Plots (a) and (b) are for the square lattice structure without source displacement and with a $\sqrt{2}a$ lateral displacement of the source position, respectively. Plots (c) and (d) are for the same structure and situations but the original permittivity of the dielectric cylinders are replaced by $\epsilon = 14 + 0.2i$.

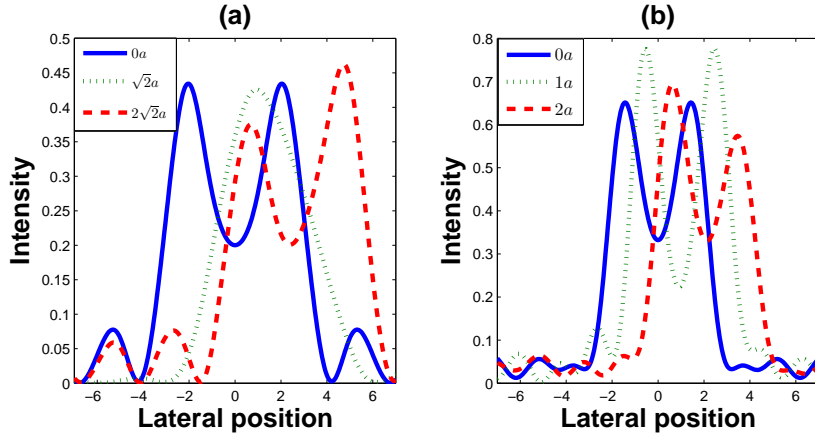


FIG. 4: Intensity distribution on the image plane for the double-source case when the center of the source-pair is shifted 0 (solid line), one lateral period (dotted line), and two lateral periods (dashed line). Results in (a) are for the square lattice case and results in (b) are for the triangular lattice case.

this curve is defined as the image strength curve. Figure 2(a) shows the results for the square lattice case having 21 cylinders along the y -direction. The peak intensity with respect to the source position reveals a inhomogeneous and non-periodic behavior (the blue o curve). We found that the periodicity of the peak strength can be improved a little bit by increasing the slab width in the lateral (y) direction. This implies that the non-periodic behavior is mainly caused by the finite lateral extension of the slab. When we replace the original slab by a wider slab (51 cylinders along y), the periodicity becomes more obvious (the green * curve). The periodicity can be further improved by including the absorption effect into the cylinders of the slab, as can be easily observed (the red x curve). This can be easily understood as follows. The absorption leads to a “finite zone”, which defines the space region that the fields around the cylinders are coupled together. If the zone is much smaller than the slab width then the “finite slab width effect” becomes unimportant, and the periodicity recovers. This “periodic but inhomogeneous” behavior implies that evanescent waves still play important role in the subwavelength imaging process even when the absorption effect has been included. According to Fig.2(b), the peak strength homogeneity is much better in the triangular lattice case than in the square lattice case. However, the periodicity of the image strength is still not obvious. The difference implies that evanescent waves are not essential in forming the image in the triangular lattice case.

Note that the source E field around the 2D point source is proportional to the Hankel function $H_0^{(1)}(k|\mathbf{r} - \mathbf{r}_s|)$, where \mathbf{r} and \mathbf{r}_s are the observation point and source point, respectively, and $k = \omega/c$ is the wave number. The Hankel function $H_0^{(1)}(\xi)$ behaves differently for $\xi \ll 1$ and $\xi \gg 1$ (See, for example, Ref.[23]), thus we can define the near field zone as the region satisfying $k|\mathbf{r} - \mathbf{r}_s| < 1$. In the near field zone the source E field has the form $A(\ln(k|\mathbf{r} - \mathbf{r}_s|/2) + \gamma)$, whereas beyond this zone the source field is approximated by $A'e^{ik|\mathbf{r} - \mathbf{r}_s|}/\sqrt{k|\mathbf{r} - \mathbf{r}_s|}$. Here A and A' are two complex constants and $\gamma \approx 0.5772$ is the Euler-Mascheroni constant. If we choose the source-slab distance (which is also the shortest distance between a cylinder and the source) as $|\mathbf{r} - \mathbf{r}_s|$ than in the square lattice case we have $k|\mathbf{r} - \mathbf{r}_s| = 0.6032 < 1$, whereas in the triangular lattice case we have $k|\mathbf{r} - \mathbf{r}_s| = 7.788 \gg 1$. It is interesting to note that for the square lattice case although the nearest cylinder of the slab is indeed within the near field zone around the source, however, the other cylinders are outside of this zone. This clearly explains why the image in this case is very sensitive to the displacement of the source. For the triangular lattice case, however, all the cylinders of the slab are outside of the near field zone, thus the displacement of the source does not influence the imaging much. We conclude that the superior imaging performance of the triangular lattice PhC slab lens is a result of the weak contribution of the near field compared to the square lattice case.

Numerical simulation results in Fig.3 can further demonstrate the above mentioned “finite slab width effect” for the square lattice structure and the “finite zone effect” for the absorptive case. Fig.3(a) is the field pattern for the (non-absorptive) 21-layer wide superlens structure, and the source is located at $y = 0$. When we move the source to $y = \sqrt{2}a$, the field pattern becomes that in Fig.3(b). It is clear that the image strength reduced and the image pattern become asymmetrical after the displacement. The “finite slab width effect” can be easily observed in Fig.3(b). For the absorptive superlens, the original dielectric cylinders are replaced by absorptive cylinders with permittivity $\epsilon = 14 + 0.2i$, and the results are shown in Fig.3(c) and 3.(d). The “finite zone effect” can be observed clearly.

Next, we consider two point sources separated by a distance which is the smallest one to maintain distinguishable images at the image plane. We keep this internal source separation fixed and shift them together along the lateral direction. In the square lattice case, the smallest distance is about 0.66λ , or $2/3$ of the wavelength. The solid curve in

Fig.4(a) shows the double-image strength on the image plane before we shift the source-pair. After shifting the sources laterally to $y = \sqrt{2}a$ (one lateral period), the two images become indistinguishable (dotted line), but distinguishable images reappear when we shift the sources to $y = 2\sqrt{2}a$ (dashed line). The subwavelength double-image resolution stability in the triangular lattices is better, as indicated in figure 4(b). Because in this case the sources and images are far from the slab, we can ensure that evanescent waves do not contribute much on the subwavelength imaging in this case.

All the results discussed above refer to point sources. However, in realistic applications, the sources must be of finite size. We have implemented numerical simulations to explore the influence of the source size on the imaging features. The finite size source in the simulations is mimicked by uniformly arranging a lot of (about 31 or so) point sources within a disk of small radius. When the source radius is smaller than one lattice constant, the conclusions concerning the single source imaging features still hold. For the situation of two sources, things become more complicated, and we have not yet got conclusive results. However, we believe this issue is worth studying because it may provide practical knowledge for designing useful devices.

III. CONCLUSION

In this paper we discuss the image quality stability of square-lattice and triangular-lattice PhC slab lenses under the influence of source movement. For square lattice slab, we found that the imaging pattern and the image peak strength are very unstable under the source movement. Coupling between evanescent waves is helpful in the subwavelength imaging but the image is sensitive to the relative position between the source and the cylinders in the front interface of the slab [17–20]. A more ideal slab lens seems to be the triangular lattice slab, in which evanescent wave do not play essential role in forming the subwavelength image, and the image quality is more stable. Thus the triangular lattice PhC slab might be a better choice for the real applications. We also found that the wider the slab in the lateral direction, the better the image periodicity, and a little absorption included can help to reduce the boundary effects of the PhC lens. We conclude that a PhC slab cannot be treated as a flat lens rigorously. We believe that a clearer understanding of these affecting factors on imaging can provide some valuable references for designing new subwavelength imaging devices.

ACKNOWLEDGEMENT

The author gratefully acknowledge financial support from National Science Council (Grant No. NSC 98-2112-M-008-114-MY3) of the Republic of China, Taiwan.

-
- [1] J.B. Pendry, “Negative Refraction Makes a Perfect Lens,” *Phys. Rev. Lett.* 85, 3966 (2000).
 - [2] Xiang Zhang and Zhaowei Liu, “Superlenses to overcome the diffraction limit,” *Nature* 435 (2008).
 - [3] Linfang Shen, Sailing He, “Studies of imaging characteristics for a slab of a lossy left hand material,” *Phys. Lett. A* 309, 298 (2003).
 - [4] Pi-Gang Luan, Hung-Da Chien, Chii-Chang Chen, Chi-Shung Tang, “Analysis on the imaging properties of a left-handed material slab”, arXiv:physics/0311122v2 (2004).
 - [5] A. N. Lagarkov and V. N. Kissel, “Near-Perfect Imaging in a Focusing System Based on a Left-Handed-Material Plate,” *Phys. Rev. Lett.* 92, 077401 (2004).
 - [6] K. Aydin, I. Bulu, and E. Ozbay, “Subwavelength resolution with a negative-index metamaterial superlens,” *Appl. Phys. Lett.* 90, 254102 (2007).
 - [7] B. D. F. Casse, W. T. Lu, Y. J. Huang, E. Gultepe, L. Menon, and S. Sridhara, “Super-resolution imaging using a three-dimensional metamaterials nanolens,” *Appl. Phys. Lett.* 96, 023114 (2010).
 - [8] Chiyan Luo, Steven G. Johnson, and J. D. Joannopoulos, and J. B. Pendry, “All-angle negative refraction without negative effective index,” *Phys. Rev. B* 65, 201104 (2002).
 - [9] E. Cubukcu, K. Aydin, and E. Ozbay, S. Foteinopolou, and C.M. Soukoulis, “Subwavelength Resolution in a Two-Dimensional Photonic-Crystal-Based Superlens,” *Phys. Rev. Lett.* 91, 207401 (2003).
 - [10] Patanjali V. Parimi, Wentao T. Lu, Plarenta Vodo, Srinivas Sridhar, “Imaging by flat lens using negative refraction,” *Nature* 426, 404 (2003).
 - [11] Zhi-Yuan Li and Lan-Lan Lin, “Evaluation of lensing in photonic crystal slabs exhibiting negative refraction,” *Phys. Rev. B* 68, 245110 (2003).
 - [12] Sailing He, Zhichao Ruan, Long Chen, and Jianqi Shen, “Focusing properties of a photonic crystal slab with negative refraction,” *Phys. Rev. B* 70, 115113 (2004).

- [13] Sanshui Xiao, Min Qiu, Zhichao Ruan, and Sailing He, "Influence of the surface termination to the point imaging by a photonic crystal slab with negative refraction," *Appl. Phys. Lett.* 85, 4269 (2004).
- [14] X Wang, Z. Ren, and K. Kempa, "Unrestricted superlensing in a triangular two dimensional photonic crystal," *Optics Express* 12, 2919-2924 (2004).
- [15] W. Belhadj, D. Gamra, F. AbdelMalek and H. Bouchriha, "Design of photonic crystal superlens with improved image resolution," *Optical and Quantum Electronics* 37, 575-586 (2005).
- [16] R. Moussa, Th. Koschny, and C. M. Soukoulis, "Excitation of surface waves in a photonic crystal with negative refraction: The role of surface termination," *Phys. Rev. B* 74, 115111 (2006).
- [17] Pi-Gang Luan; Kao-Der Chang, "Superlensing effect without obvious negative refraction", *J. Nanophotonics* 01, 013518 (2007).
- [18] A. Sukhovich et. al., "Experimental and theoretical Evidence for Subwavelength imaging in phononic crystal," *Phys. Rev. Lett.* 102,154301 (2009).
- [19] Emiliano Di Gennaro et. al., "Evidence of local effects in anomalous refraction and focusing properties of dodecagonal photonic quasicrystal," *Phys. Rev. B* 77, 193104 (2008).
- [20] Liang-Shan Chen, Chao-Hsien Kuo, and Zhen Ye, "Acoustic imaging and collimating by slabs of sonic crystals made from arrays of rigid cylinders in air," *Appl. Phys. Lett.* 85, 1072 (2004).
- [21] V. Yannopapas, *J. Phys.: Condens. Matter* 20, 255201 (2008).
- [22] V. Yannopapas and N. V. Vitanov, *phys. stat. sol. (RRL)* 2, 287 (2008).
- [23] G. B. Arfken, H. J. Weber, F. Harris, *Mathematical Methods for Physicists*, Academic Press; 5 Ed. (November 1, 2000).